Title: Enhanced Zika virus susceptibility of globally invasive *Aedes aegypti* populations

Authors: Fabien Aubry[1], Stéphanie Dabo[1], Caroline Manet[2], Igor Filipović[3], Noah H. Rose[4,5], Elliott F. Miot[1,6], Daria Martynow[1], Artem Baidaliuk[1,6], Sarah H. Merkling[1], Laura B. Dickson[1], Anna B. Crist[1], Victor O. Anyango[1], Claudia M. Romero-Vivas[7], Anubis Vega-Rúa[8], Isabelle Dusfour[9], Davy Jiolle[10,11], Christophe Paupy[10,11], Martin N. Mayanja[12], Julius J. Lutwama[12], Alain Kohl[13], Veasna Duong[14], Alongkot Ponlawat[15], Massamba Sylla[16], Jewelna Akorli[17], Sampson Otoo[17], Joel Lutomiah[18], Rosemary Sang[18], John-Paul Mutebi[19], Van-Mai Cao-Lormeau[20], Richard G. Jarman[21], Cheikh T. Diagne[22], Oumar Faye[22], Ousmane Faye[22], Amadou A. Sall[22], Carolyn S. McBride[4,5], Xavier Montagutelli[2], Gordana Rašić[3], Louis Lambrechts[1]*

Affiliations:

[1]*Insect-Virus Interactions Unit, Institut Pasteur, CNRS UMR2000, Paris, France*

[2]*Mouse Genetics Laboratory, Institut Pasteur, Paris, France*

[3]*Mosquito Control Laboratory, QIMR Berghofer Medical Research Institute, Brisbane, Australia*

[4]*Department of Ecology & Evolutionary Biology, Princeton University, Princeton, New Jersey, United States of America*

[5]*Princeton Neuroscience Institute, Princeton University, Princeton, New Jersey, United States of America*

[6]*Collège doctoral, Sorbonne Université, Paris, France*

[7]*Laboratorio de Enfermedades Tropicales, Departamento de Medicina, Fundación Universidad del Norte, Barranquilla, Colombia*

[8]*Institut Pasteur of Guadeloupe, Laboratory of Vector Control Research, Transmission Reservoir and Pathogens Diversity Unit, Morne Jolivière, Guadeloupe, France*

[9]*Vector Control and Adaptation, Institut Pasteur de la Guyane, Vectopole Amazonien Emile Abonnenc, Cayenne, French Guiana*

[10]*MIVEGEC, Montpellier University, IRD, CNRS, Montpellier, France*

[11]*Centre Interdisciplinaire de Recherches Médicales de Franceville, Franceville, Gabon*

[12]*Department of Arbovirology, Uganda Virus Research Institute, Entebbe, Uganda*

[13]*MRC-University of Glasgow Centre for Virus Research, Glasgow, United Kingdom*

[14]*Virology Unit, Institut Pasteur in Cambodia, Phnom Penh, Cambodia*

[15]*Department of Entomology, Armed Forces Research Institute of Medical Sciences, Bangkok, Thailand*

[16]*Unité d'Entomologie, de Bactériologie, de Virologie, Département de Biologie Animale, Faculté des Sciences et Techniques, Université Cheikh Anta Diop, Dakar, Senegal*

[17]*Department of Parasitology, Noguchi Memorial Institute for Medical Research, University of Ghana, Accra, Ghana*

[18]*Arbovirus/Viral Hemorrhagic Fevers Laboratory, Center for Virus Research, Kenya Medical Research Institute, Nairobi, Kenya*

[19]*Centers for Disease Control and Prevention, Fort Collins, Colorado, United States of America*

[20]*Institut Louis Malardé, Papeete, Tahiti, French Polynesia*

[21]*Viral Diseases Branch, Walter Reed Army Institute of Research, Silver Spring, Maryland, United States of America*

[22]*Institut Pasteur Dakar, Arbovirus and Viral Hemorrhagic Fevers Unit, Senegal*

*Correspondence to: louis.lambrechts@pasteur.fr

5

Abstract: The drivers and patterns of zoonotic virus emergence in the human population are poorly understood. The mosquito *Aedes aegypti* is a major arbovirus vector native to Africa that invaded most of the world's tropical belt over the past four centuries, following the evolution of a 'domestic' form that specialized in biting humans and breeding in human water-storage containers. Here, we show that human specialization and subsequent spread of *Ae. aegypti* out of Africa were accompanied by an increase in its intrinsic ability to acquire and transmit the emerging human pathogen, Zika virus. Therefore, the recent evolution and global expansion of *Ae. aegypti* promoted arbovirus emergence not solely through increased vector-host contact, but also as a result of enhanced vector susceptibility.

One Sentence Summary: Increased susceptibility of globally invasive *Ae. aegypti* populations facilitated Zika virus emergence outside Africa.

Main Text:

The mosquito *Aedes aegypti* is found throughout the tropics and sub-tropics and its range is predicted to further expand with climate change (*1*). It consists of two subspecies originally described based on morphological and ecological differences (*2*) and subsequently supported by modern population genetics (*3*). The globally invasive subspecies *Ae. aegypti aegypti* (*Aaa*) thrives in urban environments of Asia and the Americas where it oviposits in artificial containers and preferentially bites humans. The African subspecies *Ae. aegypti formosus* (*Aaf*) inhabits both urban and forest habitats of sub-Saharan Africa and bites a variety of vertebrate animals (*4, 5*). Coexistence of the two subspecies as genetically distinct entities has only been documented along the coast of Kenya, whereas in some locations of Senegal and Angola *Ae. aegypti* populations consist of a genetic blend of *Aaa* and *Aaf* (*3, 6, 7*).

The human specialist *Aaa* is thought to have evolved from generalist ancestors in Western Africa about 5,000-10,000 years ago (*6, 8*). 'Domestication' allowed the global expansion of *Aaa* during the slave-trading period (17^{th}-19^{th} centuries), which in turn fueled the first global pandemics of yellow fever and dengue (*9*). Today, *Ae. aegypti* is the most important global vector of arboviruses, including not only dengue virus (DENV) and yellow fever virus (YFV) but also newly emerging arboviruses such as Zika virus (ZIKV) and chikungunya virus (*10*). The high efficiency of *Aaa* as an arbovirus vector is generally attributed to its strong preference for humans and proclivity to lay eggs in man-made containers (*9*).

Despite ample evidence for variation in flavivirus susceptibility within and between *Ae. aegypti* populations (*11*), surprisingly little attention has been paid to the consequences of *Ae. aegypti*'s 'domestication' and global expansion out of Africa for its innate ability to acquire arbovirus infections and subsequently become infectious. A few studies in the 1970s and 1980s, motivated by the historical absence of yellow fever in Asia, ruled out the hypothesis that Asian populations of *Ae. aegypti* were inefficiently infected by YFV, however they noticed that *Aaf* populations were generally less susceptible to YFV than their *Aaa* counterparts (*12, 13*). A similar conclusion was made for DENV susceptibility (*14*), but experimental variation in virus titers of the artificial blood meals in these early studies did not allow a formal worldwide comparison.

Here, we investigated the worldwide variation of *Ae. aegypti* susceptibility to ZIKV infection using a panel of 14 laboratory colonies recently established (2-16 laboratory generations) from field-collected specimens (Table S1). ZIKV is a flavivirus (family: *Flaviviridae*) first isolated from a sentinel monkey in Uganda in 1947 (*15*) and mainly transmitted among humans by *Ae. aegypti*. The first reported human epidemic of ZIKV occurred in 2007 on the Pacific island of Yap, Micronesia (*16*). Subsequently, larger ZIKV outbreaks were recorded in French Polynesia and other Pacific islands during 2013-2014 (*17*). In 2015, ZIKV was detected in Brazil from where it rapidly spread across the Americas and the Caribbean, causing hundreds of thousands of human cases (*18*). The factors underlying the explosiveness and magnitude of ZIKV emergence in the Pacific and the Americas are still poorly understood. Reciprocally, the lack of major human epidemics of ZIKV in regions with seemingly favorable conditions, such as Africa or continental Asia, remains largely unexplained to date (*18*).

To compare ZIKV susceptibility between our *Ae. aegypti* colonies, we generated empirical dose-response curves based on a standardized membrane-feeding assay (Fig. S1A). Dose-response curves account for the strong dose-dependency of infection success (*19, 20*) and provide an absolute measure of susceptibility, which can be summarized by the virus dose infecting 50% of blood-fed mosquitoes (50% oral infectious dose; OID_{50}). Multiple blood meals are known to enhance systemic virus dissemination in ZIKV-infected *Ae. aegypti* but they do not affect initial infection prevalence (*21*), therefore a single infectious blood meal is adequate to obtain relevant OID_{50} estimates. Because ZIKV susceptibility is also influenced by the virus strain (*20, 22*), we used a panel of seven wild-type ZIKV strains encompassing the current viral genetic diversity (Table S2).

We first measured ZIKV susceptibility in a worldwide panel of eight *Ae. aegypti* colonies (Table S1) originating from Africa (Cameroon, Uganda, Gabon), the Americas (Colombia, Guadeloupe, French Guiana) and Asia (Thailand, Cambodia). We individually scored the infection status of 3,113 female *Ae. aegypti* following oral exposure to three different infectious doses of six ZIKV strains. The infection status depended on a three-way interaction between infectious dose, ZIKV strain and mosquito population (multivariate logistic regression: p=0.0238), indicating that the dose-response curves differed significantly among virus-population pairs (Fig. 1A). When mosquito populations were nested within their continent of origin (Asia, Africa, Americas) in the statistical model, there was a strong effect of the continent (p<0.0001), which was mainly driven by the significantly lower ZIKV susceptibility of the three African mosquito populations. Across the ZIKV strains, the OID_{50} estimates (Table S3) ranged from 6.3 to 8.1 $\log_{10}$ FFU/ml for the three African populations and from 4.7 to 6.8 $\log_{10}$ FFU/ml for the five non-African populations

(Fig. 1B). We confirmed that variation in ZIKV susceptibility did not simply reflect differences in colonization history between the mosquito populations. We analyzed the OID_{50} estimates as a function of the average number of generations spent in the laboratory and found no statistical support for an effect of the generation (analysis of variance [ANOVA]: p=0.8236), or an interaction effect between the ZIKV strain and the generation (ANOVA: p=0.8618).

The three African colonies of our worldwide panel were significantly less susceptible to ZIKV infection than their non-African counterparts, however they did not represent the full extent of *Ae. aegypti* genetic diversity in the ancestral range of the species (*6*). These three colonies came from places expected to harbor relatively pure *Aaf* populations, whereas other African populations from the Sahelian region show signatures of mixed ancestry with globally invasive *Aaa* (*7, 8*). To expand our assessment of African *Ae. aegypti* populations, we examined a panel of six additional mosquito colonies (Table S1) originating from Senegal (NGO, KED), Ghana (KUM), Uganda (ENT) and Kenya (KAK, RAB) (*7*). We measured their ZIKV susceptibility with our standardized membrane-feeding assay and the colonies from Gabon and Guadeloupe of our worldwide panel were included as references (Fig. 2A). The six African colonies differed significantly in their dose response to the ZIKV_Cambodia_2010 strain (multivariate logistic regression excluding reference colonies: p<0.0001; n=271), but not to the ZIKV_Senegal_2011 strain (p=0.0587; n=363). The OID_{50} estimates (Table S3) ranged from 6.3 (NGO) to 7.9 (KED) log_{10} FFU/ml for the ZIKV_Cambodia_2010 strain and from 4.9 (NGO) to 6.2 (KED) log_{10} FFU/ml for the ZIKV_Senegal_2011 strain (Fig. 2B). There was no evidence for an effect of the laboratory generation (ANOVA: p=0.7399) or an interaction effect between the ZIKV strain and the laboratory generation (ANOVA: p=0.9236) on the OID_{50} estimates. Although the

ZIKV_Senegal_2011 strain was more infectious overall, we noticed that for both virus strains the most and least susceptible African colonies were the same (NGO and KED, respectively). These two colonies are expected to differ genetically according to a recent study that analyzed the whole-genome sequences of their wild progenitors (*7*). In that study, ADMIXTURE analysis identified three genomic clusters (East Africa, Central/West Africa, and globally invasive 'domestic' ancestry components) and detected a variable level of 'domestic' ancestry in several African *Ae. aegypti* populations. For instance, the average proportion of 'domestic' ancestry in the wild progenitors was 37.4% for NGO and 0.86% for KED (*7*). We thus analyzed ZIKV susceptibility as a function of the level of 'domestic' ancestry and found that they were positively associated (Fig. 2C), both for the ZIKV_Cambodia_2010 strain (square root regression: p=0.0047; R^2=0.761) and for the ZIKV_Senegal_2011 strain (square root regression: p=0.0437; R^2=0.519). When omitting the pure *Aaa* reference population from Guadeloupe, the relationship was still significant for the ZIKV_Cambodia_2010 strain (linear regression: p=0.0047; R^2=0.824) but no longer for the ZIKV_Senegal_2011 strain (linear regression: p=0.1189; R^2=0.414). These results provide further evidence for the higher ZIKV susceptibility of the 'domestic' subspecies *Aaa* relative to the African subspecies *Aaf*.

To investigate the genetic basis of *Ae. aegypti* worldwide variation in ZIKV susceptibility, we intercrossed the colony from Guadeloupe (susceptible parent; 100% *Aaa*) with the colony from Gabon (resistant parent; 7.3% *Aaa*) to perform quantitative trait locus (QTL) mapping by bulk segregant analysis (Fig. S2). In two reciprocal intercrosses, F_1 hybrids displayed a level of susceptibility to the ZIKV_Cambodia_2010 strain that was intermediate but closer to the resistant parent (Fig. 3A), suggesting that resistant alleles were partially dominant. The level of

ZIKV susceptibility remained intermediate during the following five generations of both intercrosses (Fig. 3A). After three generations of recombination, we genotyped phenotypic pools of the F_4 progeny based on their ZIKV-resistant (uninfected) or ZIKV-susceptible (infected) phenotype (2 replicate pools of 48 individuals per phenotype). We used a total of ~230,000 single-nucleotide polymorphisms identified on a genome-wide scale by restriction site-associated DNA sequencing to detect deviations in allele frequencies between ZIKV-resistant and ZIKV-susceptible pools. In the first intercross (Guadeloupe males × Gabon females), we detected a cluster of five highly significant QTL associated with infection status (false discovery rate [FDR]<0.001) located between 128.3 Mb and 282.7 Mb on chromosome 2 (Fig. 3B; Table S4). In the second intercross (Gabon males × Guadeloupe females), we also detected four QTL associated with infection status albeit with lower statistical support (FDR<0.05) between 37.0 Mb and 344.8 Mb on chromosome 2 (Fig. 3C; Table S4). In both intercrosses there was a complete lack of genotype-phenotype association signal on chromosomes 1 and 3 (Fig. 3B-C). The strongest QTL signals on chromosome 2 were distinct between the two intercrosses, which could reflect incomplete detection power and/or causative variants that are not fixed differences between the parental populations (*23*). Earlier genetic mapping studies of DENV susceptibility in *Ae. aegypti* also yielded different QTL sets in separate crosses, including QTL located at different positions of chromosome 2 (*24, 25*). Analyses of ancestry differences confirmed that in both intercrosses the significant QTL corresponded to an enrichment of the resistant parental genome in the resistant progeny (Fig. S3). Although our QTL mapping approach had a relatively low resolution due to the limited number of unique recombination events captured in only three generations, it provided clear evidence that the difference in ZIKV susceptibility between the Gabon and Guadeloupe colonies is governed by one or more genetic loci on chromosome 2.

Finally, we evaluated the significance of the observed difference in ZIKV susceptibility between *Aaa* and *Aaf* for transmission potential in a mouse model of ZIKV infection. Artificial infectious blood meals are a convenient proxy but they do not necessarily recapitulate the complexity of a blood meal taken on a live host, which potentially contains host factors and viral antigens that may influence virus acquisition by mosquitoes (*26-28*). In addition, infection probability is only one component of the virus transmission process, which also requires systemic dissemination and viral release in mosquito saliva (*11*). To address the limitations of artificial blood meals, we compared the cumulative amount of virus transmission between the Gabon and Guadeloupe colonies when mosquitoes acquired infection from a live host. Groups of mosquitoes from both colonies were allowed to simultaneously blood feed on the same ZIKV-infected mice (Fig. S1B). Following intra-peritoneal injection of the ZIKV_Cambodia_2010 strain, immunocompromised mice (*Ifnar1*$^{-/-}$) from two genetic backgrounds (C57BL/6J and 129S2/SvPas) developed viremia that peaked 2-3 days post infection and was detectable in plasma for about one week (Fig. 4). Across the mouse viremic period, the proportion of infected (ZIKV-positive body) and infectious (ZIKV-positive saliva) mosquitoes roughly followed the kinetics of plasma viremia but was strikingly lower for Gabon than for Guadeloupe mosquitoes (Fig. 4). Accounting for differences between replicate mice, infection rate was significantly lower (multivariate logistic regression: $p<0.0392$) for the Gabon mosquitoes at all time points, with the exception of day 2 post mouse infection in the C57BL/6J strain ($p=0.0898$) and day 5 post mouse infection in the 129S2/SvPas strain ($p=0.2976$). Likewise, the proportion of infectious mosquitoes was significantly lower ($p<0.0176$) for the Gabon colony on days 2 and 3 post mouse infection in both mouse strains, as well as on days 1 and 5 post mouse infection ($p<0.0305$) in the C57BL/6J strain. Therefore, the

large difference in ZIKV susceptibility previously observed with artificial infectious blood meals translated into a substantially lower potential to transmit ZIKV of *Aaf* relative to *Aaa*.

Together, our results indicate that 'domestication' of *Ae. aegypti* about 5,000-10,000 years ago (*6, 8*) was accompanied by an increase in its innate ability to acquire and transmit ZIKV. Today, some African populations of *Ae. aegypti* such as NGO in Western Senegal display morphological, behavioral and genetic features typical of *Aaa* populations outside Africa (*7*), as does their ZIKV susceptibility. This is consistent with an earlier study in Senegal reporting a cline in the relative abundance of *Aaa* and *Aaf* (based on morphological features) that correlated with variation in DENV susceptibility (*29*). Whether the differential ZIKV susceptibility between *Aaa* and *Aaf* extend to other flaviviruses than ZIKV remains to be ascertained. Experimental infections of the *Ae. aegypti* colonies from our worldwide panel with YFV (Fig. S4) and DENV (Fig. S5) showed a similar pattern as for ZIKV. These data are consistent with a higher genetic resistance of *Aaf* against flaviviruses in general, however without a broader panel of YFV and DENV strains we cannot rule out the existence of strain-specific interactions (*30*). It is unlikely that increased ZIKV susceptibility of the globally invasive *Aaa* subspecies was driven by relaxed natural selection because arboviruses apparently do not represent a meaningful selective force on mosquito populations (*31*). Moreover, ZIKV usually circulates in sylvatic cycles that involve other mosquito species than *Ae. aegypti* (*32*), reducing opportunities for natural selection to act. We speculate that increased susceptibility was a by-product of adaptation to the 'domestic' lifestyle due to genetic drift and/or genetic linkage between 'domestic' genes and susceptibility genes, but this remains to be tested. This hypothesis is supported by the overlap between the most significant ZIKV susceptibility QTL spanning from 128 to 189 Mb on

chromosome 2 and a previously identified genomic hotspot for human specialization between 133 and 168 Mb on the same chromosome (*7*). For example, the human-preferring NGO population shows higher levels of genetic differentiation from animal-preferring populations and elevated levels of 'domestic' ancestry in this genomic region (up to 50% vs. the 37.4% genome-wide average).

Regardless of the underlying evolutionary mechanism, the marked difference in ZIKV susceptibility between *Aaa* and *Aaf* may help to explain one puzzling aspect of Zika epidemiology. Although ZIKV was first isolated in Uganda and is known to be present across most of Africa, it has yet to cause large-scale human outbreaks on this continent (*33, 34*). Arbovirus emergence is primarily driven by urbanization, globalization and the failure of prevention measures, and the risk is further modulated by region-specific factors such as the immune and genetic background of human populations (*35, 36*). The low seroprevalence of neutralizing antibodies against ZIKV typically observed in Africa (*37-39*) makes it unlikely that herd immunity is the main factor preventing ZIKV outbreaks. Our findings suggest that instead the lower transmission potential of *Aaf* could have hindered ZIKV emergence on the African continent. This explanation is consistent with the few examples of ZIKV circulation in human populations of Africa, and points to opportunities for experimental confirmation with additional mosquito samples. ZIKV was detected in Gabon in 2007 but the vector was presumably another mosquito species, *Aedes albopictus* (*40*). ZIKV circulated during 2016-2017 in Angola (*41*) but a recent study found that an *Ae. aegypti* population from Luanda, Angola consisted of a genetic mixture of *Aaa* and *Aaf* (*6*). Possibly, a similar situation could have facilitated the large ZIKV outbreak that occurred in Cape Verde during 2015-2016 (*42*), based on the untested assumption

that the local *Ae. aegypti* population there harbors a large proportion of 'domestic' ancestry similar to the nearby populations of Western Senegal. We conclude that the evolution of human specialization and subsequent spread of *Ae. aegypti* out of Africa may have promoted arbovirus emergence not solely through increased vector-host contact, but also as a result of enhanced vector permissiveness.

References and Notes:

1. M. U. G. Kraemer *et al.*, Past and future spread of the arbovirus vectors Aedes aegypti and Aedes albopictus. *Nat Microbiol* **4**, 854-863 (2019).
2. P. F. Mattingly, Genetical aspects of the Aedes aegypti problem. I. Taxonomy and bionomics. *Ann Trop Med Parasitol* **51**, 392-408 (1957).
3. A. Gloria-Soria *et al.*, Global genetic diversity of Aedes aegypti. *Mol Ecol* **25**, 5377-5395 (2016).
4. J. E. Brown *et al.*, Worldwide patterns of genetic differentiation imply multiple 'domestications' of Aedes aegypti, a major vector of human diseases. *Proc Biol Sci* **278**, 2446-2454 (2011).
5. C. S. McBride, Genes and Odors Underlying the Recent Evolution of Mosquito Preference for Humans. *Curr Biol* **26**, R41-46 (2016).
6. P. Kotsakiozi *et al.*, Population structure of a vector of human diseases: Aedes aegypti in its ancestral range, Africa. *Ecol Evol* **8**, 7835-7848 (2018).
7. N. H. Rose *et al.*, Climate and Urbanization Drive Mosquito Preference for Humans. *Curr Biol*, (2020). Online ahead of print: https://doi.org/10.1016/j.cub.2020.06.092

8. J. E. Crawford *et al.*, Population genomics reveals that an anthropophilic population of Aedes aegypti mosquitoes in West Africa recently gave rise to American and Asian populations of this major disease vector. *BMC Biol* **15**, 16 (2017).

9. O. J. Brady, S. I. Hay, The Global Expansion of Dengue: How Aedes aegypti Mosquitoes Enabled the First Pandemic Arbovirus. *Annu Rev Entomol*, 191-208 (2020).

10. S. C. Weaver, C. Charlier, N. Vasilakis, M. Lecuit, Zika, Chikungunya, and Other Emerging Vector-Borne Viral Diseases. *Annu Rev Med* **69**, 395-408 (2018).

11. W. C. Black *et al.*, Flavivirus susceptibility in Aedes aegypti. *Arch Med Res* **33**, 379-388 (2002).

12. T. H. Aitken, W. G. Downs, R. E. Shope, Aedes aegypti strain fitness for yellow fever virus transmission. *Am J Trop Med Hyg* **26**, 985-989 (1977).

13. W. J. Tabachnick *et al.*, Oral infection of Aedes aegypti with yellow fever virus: geographic variation and genetic considerations. *Am J Trop Med Hyg* **34**, 1219-1224 (1985).

14. D. J. Gubler, S. Nalim, R. Tan, H. Saipan, J. Sulianti Saroso, Variation in susceptibility to oral infection with dengue viruses among geographic strains of Aedes aegypti. *Am J Trop Med Hyg* **28**, 1045-1052 (1979).

15. G. W. Dick, S. F. Kitchen, A. J. Haddow, Zika virus. I. Isolations and serological specificity. *Trans R Soc Trop Med Hyg* **46**, 509-520 (1952).

16. M. R. Duffy *et al.*, Zika virus outbreak on Yap Island, Federated States of Micronesia. *N Engl J Med* **360**, 2536-2543 (2009).

17. D. Musso, E. J. Nilles, V. M. Cao-Lormeau, Rapid spread of emerging Zika virus in the Pacific area. *Clin Microbiol Infect* **20**, O595-596 (2014).

18. D. Musso, A. I. Ko, D. Baud, Zika Virus Infection - After the Pandemic. *N Engl J Med* **381**, 1444-1457 (2019).

19. A. T. Ciota *et al.*, Effects of Zika Virus Strain and Aedes Mosquito Species on Vector Competence. *Emerg Infect Dis* **23**, 1110-1117 (2017).

20. C. M. Roundy *et al.*, Variation in Aedes aegypti Mosquito Competence for Zika Virus Transmission. *Emerg Infect Dis* **23**, 625-632 (2017).

21. P. M. Armstrong *et al.*, Successive blood meals enhance virus dissemination within mosquitoes and increase transmission potential. *Nat Microbiol* **5**, 239-247 (2020).

22. E. Calvez *et al.*, Differential transmission of Asian and African Zika virus lineages by Aedes aegypti from New Caledonia. *Emerg Microbes Infect* **7**, 159 (2018).

23. H. Bastide, J. D. Lange, J. B. Lack, A. Yassin, J. E. Pool, A Variable Genetic Architecture of Melanic Evolution in Drosophila melanogaster. *Genetics* **204**, 1307-1319 (2016).

24. C. F. Bosio, R. E. Fulton, M. L. Salasek, B. J. Beaty, W. C. Black, Quantitative trait loci that control vector competence for dengue-2 virus in the mosquito Aedes aegypti. *Genetics* **156**, 687-698 (2000).

25. C. Gomez-Machorro, K. E. Bennett, M. del Lourdes Munoz, W. C. Black, Quantitative trait loci affecting dengue midgut infection barriers in an advanced intercross line of Aedes aegypti. *Insect Mol Biol* **13**, 637-648 (2004).

26. Y. Liu *et al.*, Evolutionary enhancement of Zika virus infectivity in Aedes aegypti mosquitoes. *Nature* **545**, 482-486 (2017).

27. N. Nguyen *et al.*, Host and viral features of human dengue cases shape the population of infected and infectious Aedes aegypti mosquitoes. *Proc Natl Acad Sci U S A* **110**, 9072-9077 (2013).

28. Y. Zhu *et al.*, Host serum iron modulates dengue virus acquisition by mosquitoes. *Nat Microbiol* **4**, 2405-2415 (2019).

29. M. Sylla, C. Bosio, L. Urdaneta-Marquez, M. Ndiaye, W. C. Black, Gene flow, subspecies composition, and dengue virus-2 susceptibility among Aedes aegypti collections in Senegal. *PLoS Negl Trop Dis* **3**, e408 (2009).

30. L. B. Dickson, I. Sanchez-Vargas, M. Sylla, K. Fleming, W. C. Black, Vector competence in West African Aedes aegypti Is Flavivirus species and genotype dependent. *PLoS Negl Trop Dis* **8**, e3153 (2014).

31. L. Lambrechts, M. C. Saleh, Manipulating Mosquito Tolerance for Arbovirus Control. *Cell Host Microbe* **26**, 309-313 (2019).

32. G. Gutierrez-Bugallo *et al.*, Vector-borne transmission and evolution of Zika virus. *Nat Ecol Evol* **3**, 561-569 (2019).

33. A. G. Buchwald, M. H. Hayden, S. K. Dadzie, S. H. Paull, E. J. Carlton, Aedes-borne disease outbreaks in West Africa: A call for enhanced surveillance. *Acta Trop*, 105468 (2020).

34. D. Weetman *et al.*, Aedes Mosquitoes and Aedes-Borne Arboviruses in Africa: Current and Future Threats. *Int J Environ Res Public Health* **15**, 220 (2018).

35. H. Ketkar, D. Herman, P. Wang, Genetic Determinants of the Re-Emergence of Arboviral Diseases. *Viruses* **11**, 150 (2019).

36. A. Wilder-Smith *et al.*, Epidemic arboviral diseases: priorities for research and public health. *Lancet Infect Dis* **17**, e101-e106 (2017).

37. J. T. Kayiwa *et al.*, Confirmation of Zika virus infection through hospital-based sentinel surveillance of acute febrile illness in Uganda, 2014-2017. *J Gen Virol* **99**, 1248-1252 (2018).

38. A. C. Willcox *et al.*, Seroepidemiology of Dengue, Zika, and Yellow Fever Viruses among Children in the Democratic Republic of the Congo. *Am J Trop Med Hyg* **99**, 756-763 (2018).

39. B. Kisuya, M. M. Masika, E. Bahizire, J. O. Oyugi, Seroprevalence of Zika virus in selected regions in Kenya. *Trans R Soc Trop Med Hyg* **113**, 735-739 (2019).

40. G. Grard *et al.*, Zika virus in Gabon (Central Africa)--2007: a new threat from Aedes albopictus? *PLoS Negl Trop Dis* **8**, e2681 (2014).

41. S. C. Hill *et al.*, Emergence of the Asian lineage of Zika virus in Angola: an outbreak investigation. *Lancet Infect Dis* **19**, 1138-1147 (2019).

42. O. Faye *et al.*, Genomic Epidemiology of 2015-2016 Zika Virus Outbreak in Cape Verde. *Emerg Infect Dis* **26**, 1084-1090 (2020).

43. M. U. Kraemer *et al.*, The global distribution of the arbovirus vectors Aedes aegypti and Ae. albopictus. *eLife* **4**, e08347 (2015).

44. B. N. Mansfeld, R. Grumet, QTLseqr: An R Package for Bulk Segregant Analysis with Next-Generation Sequencing. *Plant Genome* **11**, 1-5 (2018).

45. L. B. Dickson *et al.*, Diverse laboratory colonies of Aedes aegypti harbor the same adult midgut bacterial microbiome. *Parasites Vectors* **11**, 207 (2018).

46. A. Baidaliuk *et al.*, Cell-Fusing Agent Virus Reduces Arbovirus Dissemination in Aedes aegypti Mosquitoes In Vivo. *J Virol* **93**, e00705-19 (2019).

47. A. Fontaine, D. Jiolle, I. Moltini-Conclois, S. Lequime, L. Lambrechts, Excretion of dengue virus RNA by Aedes aegypti allows non-destructive monitoring of viral dissemination in individual mosquitoes. *Sci Rep* **6**, 24885 (2016).

48. T. Fansiri *et al.*, Genetic Mapping of Specific Interactions between Aedes aegypti Mosquitoes and Dengue Viruses. *PLoS Genet* **9**, e1003621 (2013).

49. M. Caron *et al.*, First evidence of simultaneous circulation of three different dengue virus serotypes in Africa. *PLoS ONE* **8**, e78030 (2013).

50. E. Chungue *et al.*, Molecular epidemiology of dengue-1 and dengue-4 viruses. *J Gen Virol* **76**, 1877-1884 (1995).

51. F. Rodhain, C. Hannoun, F. X. Jousset, P. Ravisse, [Isolation of the yellow fever virus in Paris from 2 imported human cases]. *Bull Soc Pathol Exot Filiales* **72**, 411-415 (1979).

52. T. H. G. Aitken, An in vitro feeding technique for artificially demonstrating virus transmission by mosquitoes. *Mosq News* **37**, 130-133 (1977).

53. G. Rasic, I. Filipovic, A. R. Weeks, A. A. Hoffmann, Genome-wide SNPs lead to strong signals of geographic structure and relatedness patterns in the major arbovirus vector, Aedes aegypti. *BMC Genomics* **15**, 275 (2014).

54. B. K. Peterson, J. N. Weber, E. H. Kay, H. S. Fisher, H. E. Hoekstra, Double digest RADseq: an inexpensive method for de novo SNP discovery and genotyping in model and non-model species. *PLoS ONE* **7**, e37135 (2012).

55. B. J. Matthews *et al.*, Improved reference genome of Aedes aegypti informs arbovirus vector control. *Nature* **563**, 501-507 (2018).

56. B. Langmead, C. Trapnell, M. Pop, S. L. Salzberg, Ultrafast and memory-efficient alignment of short DNA sequences to the human genome. *Genome Biol* **10**, R25 (2009).

57. H. Li *et al.*, The Sequence Alignment/Map format and SAMtools. *Bioinformatics* **25**, 2078-2079 (2009).

58. T. S. Korneliussen, A. Albrechtsen, R. Nielsen, ANGSD: Analysis of Next Generation Sequencing Data. *BMC Bioinformatics* **15**, 356 (2014).

59. P. M. Magwene, J. H. Willis, J. K. Kelly, The statistics of bulk segregant analysis using next generation sequencing. *PLoS Comput Biol* **7**, e1002255 (2011).

60. N. Patterson *et al.*, Ancient admixture in human history. *Genetics* **192**, 1065-1093 (2012).

61. H. Wickham, *ggplot2: Elegant Graphics for Data Analysis* (Springer-Verlag, New York, 2016).

62. J. Fox, S. Weisberg, *An R Companion to Applied Regression* (Sage, Thousand Oaks, CA, ed. Third, 2019).

Acknowledgments: We thank Catherine Lallemand for assistance with mosquito rearing and the Institut Pasteur animal facility staff for the breeding of *Ifnar1*$^{-/-}$ mice. We thank the volunteers and the ICAReB staff for the human blood supply. We are grateful to Anna-Bella Failloux for sharing the YFV strain. **Funding:** This work was primarily funded by the European Union's Horizon 2020 research and innovation programme under ZikaPLAN grant agreement no. 734584 (to LL). This work was also supported by Agence Nationale de la Recherche (grants ANR-16-CE35-0004-01, ANR-17-ERC2-0016-01 and ANR-18-CE35-0003-01 to LL), the French Government's Investissement d'Avenir program Laboratoire d'Excellence Integrative Biology of Emerging Infectious Diseases (grant ANR-10-LABX-62-IBEID to LL and XM), the Inception

program (Investissement d'Avenir grant ANR-16-CONV-0005 to LL), the City of Paris Emergence(s) program in Biomedical Research (to LL), the QIMR Berghofer Medical Research Institute (Seed Funding Grant to GR), the Programme Opérationnel FEDER-Guadeloupe-Conseil Régional 2014-2020 (grant 2015-FED-192 to AVR), the European Union's Horizon 2020 Research and innovation programme under "ZIKALLIANCE" grant agreement no. 734548 (to AV-R), the US National Institutes of Health (grant NIDCD R00-DC012069 to CSM), a Helen Hay Whitney Postdoctoral Fellowship (to NHR), the UK Medical Research Council (grant MC_UU_12014/8 to AK) and the CDC (J-PM). CSM is a New York Stem Cell Foundation – Robertson Investigator. The funders had no role in study design, data collection and interpretation, or the decision to submit the work for publication. **Author contributions:** FA and LL designed and coordinated the study. FA, SD, CM, EFM, DM, AB, SHM, LBD, ABC and VOA performed the mosquito experiments. IF and GR generated and analyzed the RAD-seq data and performed the QTL mapping. NHR performed the admixture analyses. NHR, CMR-V, AV-R, ID, DJ, CP, MNM, JJL, AK, VD, AP, MS, JA, SO, JL, RS, J-PM and CSM performed field collections to initiate mosquito colonies. V-MC-L, RGJ, CTD, OumF, OusF and AAS obtained the virus isolates and organized their transfer. NHR and CSM coordinated the collection and the maintenance of the African mosquito panel. FA, CM, XM and LL designed and implemented the mouse-to-mosquito transmission assay. FA and LL wrote and revised the manuscript with input from all other authors. **Competing interests:** Authors declare no competing interests. **Data and materials availability:** Raw sequencing data were deposited to the SRA repository under accession number PRJNA640190. All other raw data are available from the Zenodo repository at https://doi.org/10.5281/zenodo.3981206. Sharing some of the materials is subject to material transfer agreements with Institut Louis Malardé, Institut Pasteur Dakar, Princeton University,

Universidad del Norte, Walter Reed Army Institute of Research, and the World Reference Center for Emerging Viruses and Arboviruses.

Supplementary Materials:

Materials and Methods

Figures S1-S5

Tables S1-S4

References (*45-62*)

Figure Legends:

Fig. 1. Native populations of *Ae. aegypti* in Africa are less susceptible to ZIKV than globally invasive populations outside Africa. **A**. Dose-response curves of eight field-derived *Ae. aegypti* colonies challenged by six low-passage ZIKV strains. The proportions of ZIKV-infected mosquitoes 7 days post oral challenge are shown as a function of the blood meal titers in log_{10}-transformed focus-forming units (FFU)/ml. Each box represents a different ZIKV strain as labeled at the top. The logistic regression lines are color-coded for the different mosquito populations. **B**. Geographical origins of the eight *Ae. aegypti* colonies and their estimated OID_{50} values expressed in log_{10} FFU/ml for the six low-passage ZIKV strains tested in panel A. The pie charts show the six OID_{50} values estimated from the dose-response curves shown in panel A (clockwise from the top: ZIKV_Senegal_2015, ZIKV_Cambodia_2010, ZIKV_Thailand_2014, ZIKV_Philippines_2012, ZIKV_Puerto_Rico_2015, ZIKV_F_Polynesia_2013) and represented on a color scale (except for the undetermined OID_{50} values shown in grey). The grey background indicates the approximate distribution of *Ae. aegypti* (*43*). The light grey represents the globally invasive subspecies *Aaa* whereas the dark grey represents the African subspecies *Aaf*.

Fig. 2. ZIKV susceptibility among African populations of *Ae. aegypti* correlates positively with their proportion of 'domestic' genetic ancestry. **A**. Dose-response curves of eight field-derived *Ae. aegypti* colonies challenged by two low-passage ZIKV strains. Colonies from Gabon and Guadeloupe are the same as in the worldwide panel shown in Fig. 1 and served as resistant and susceptible references, respectively. The other six colonies were derived from a panel of African populations sampled in a separate study (*7*) and abbreviated as follows: NGO=Ngoye, Senegal; KED=Kédougou, Senegal; KUM=Kumasi, Ghana; ENT=Entebbe, Uganda; KAK=Kakamega,

Kenya; RAB=Rabai, Kenya. The proportions of ZIKV-infected mosquitoes 7 days post oral challenge are shown as a function of the blood meal titers in log_{10}-transformed focus-forming units (FFU)/ml. Each box represents a different ZIKV strain as labeled at the top. The logistic regression lines are color-coded for the different mosquito populations. **B**. Geographical origins of the seven African *Ae. aegypti* colonies and their estimated OID_{50} values expressed in log_{10} FFU/ml for the two low-passage ZIKV strains tested in panel A. The pie charts show the OID_{50} values estimated from the dose-response curves (left: ZIKV_Cambodia_2010; right: ZIKV_Senegal 2011) and represented on a color scale. The grey shading indicates the approximate distribution of *Ae. aegypti* (*43*). **C**. Relationship between ZIKV susceptibility of the colonies and the average proportion of 'domestic' genetic ancestry of their wild-caught founders, inferred by ADMIXTURE analyses (*7*). Note that ZIKV susceptibility is represented by OID_{50} estimates for ZIKV_Cambodia_2010 and by OID_{75} estimates for ZIKV_Senegal_2011 because of the higher overall infectiousness of the latter strain. Each box represents a different ZIKV strain as labeled at the top. The black lines represent the square root regression results for the ZIKV_Cambodia_2010 strain (R^2=0.761; p=0.0047) and the ZIKV_Senegal_2011 strain (R^2=0.519; p=0.0437). The best-fit regression function was obtained by comparing R^2 values between various regression models.

Fig. 3. Genetic analysis of intercrossed African and non-African mosquitoes identifies genomic regions underlying ZIKV susceptibility. **A**. Dose-response curves of the parental colonies and the F_1, F_2, F_3 and F_6 generations of intercross 1 (Guadeloupe males × Gabon females) and intercross 2 (Gabon males × Guadeloupe females) orally challenged with the ZIKV_Cambodia_2010 strain. The percentage of ZIKV-infected mosquitoes 7 days post oral challenge is shown as a

function of the blood meal titers in log_{10}-transformed focus-forming units (FFU)/ml. Each box represents a different intercross generation, as labeled at their top, and the lines represent the logistic regression results. **B**-**C**. QTL mapping results obtained for the F_4 generation of intercross 1 (**B**) and intercross 2 (**C**). The statistical significance of the genotype-phenotype association, averaged by 5-Mb moving windows, is shown along the three chromosomes. The horizontal red lines indicate the 0.1% (**B**) and 5% (**C**) genome-wide false discovery rate (FDR) thresholds calculated with the Benjamini-Hochberg method implemented in QTLseqr (*44*).

Fig. 4. African mosquitoes have less potential than non-African mosquitoes to acquire and transmit ZIKV from a viremic host. Mouse-to-mosquito transmission of ZIKV was evaluated in immunocompromised (*Ifnar1*$^{-/-}$) C57BL/6J (**A**) and 129S2/SvPas (**B**) mouse strains. The graphs show the time course of mouse plasma viremia (infectious titers expressed in log_{10}-transformed focus-forming units [FFU]/ml, top graph), mosquito infection (percentage of ZIKV-infected mosquitoes 14 days post blood meal, middle graph) and mosquito infectiousness (percentage of mosquitoes with ZIKV-positive saliva 14 days post blood meal, bottom graph) during the mouse viremic period. In all panels, each line represents one of three replicate mice, identified by different symbols. In the middle and bottom graphs, each data point represents a group of 2-20 (median 11) mosquitoes. The blue and red colors represent mosquitoes from Guadeloupe and Gabon, respectively.

Science
AAAS

Supplementary Materials for

Enhanced Zika virus susceptibility of globally invasive *Aedes aegypti* populations

Fabien Aubry, Stéphanie Dabo, Caroline Manet, Igor Filipović, Noah H. Rose, Elliott F. Miot, Daria Martynow, Artem Baidaliuk, Sarah H. Merkling, Laura B. Dickson, Anna B. Crist, Victor O. Anyango, Claudia M. Romero-Vivas, Anubis Vega-Rúa, Isabelle Dusfour, Davy Jiolle, Christophe Paupy, Martin N. Mayanja, Julius J. Lutwama, Alain Kohl, Veasna Duong, Alongkot Ponlawat, Massamba Sylla, Jewelna Akorli, Sampson Otoo, Joel Lutomiah, Rosemary Sang, John-Paul Mutebi, Van-Mai Cao-Lormeau, Richard G. Jarman, Cheikh T. Diagne, Oumar Faye, Ousmane Faye, Amadou A. Sall, Carolyn S. McBride, Xavier Montagutelli, Gordana Rašić, Louis Lambrechts

Correspondence to: louis.lambrechts@pasteur.fr

This PDF file includes:

Materials and Methods

Ethics and regulatory information

This study used human blood samples to prepare mosquito artificial infectious blood meals. For that purpose, healthy blood donor recruitment was organized by the local investigator assessment using medical history, laboratory results and clinical examinations. Biological samples were supplied through the participation of healthy adult volunteers at the ICAReB biobanking platform (BB-0033-00062/ICAReB platform/Institut Pasteur, Paris/BBMRI AO203/[BIORESOURCE]) of the Institut Pasteur in the CoSImmGen and Diagmicoll protocols, which had been approved by the French Ethical Committee Ile-de-France I. The Diagmicoll protocol was declared to the French Research Ministry under reference 343 DC 2008-68 COL 1. All adult subjects provided written informed consent. The mouse experiments were approved by the Institut Pasteur Animal Ethics Committee (project number dap170045) and authorized by the French Ministry of Research (authorization number 12861). The Institut Pasteur animal facility had received accreditation from the French Ministry of Agriculture to perform experiments on live animals in compliance with the French and European regulations on the care and protection of laboratory animals (authorization number 75-15-01). Mosquito eggs were collected and exported with the permission from local institutions and/or governments as required (Kenya SERU No. 3433; Gabon AR0020/14/MESR/CENAREST/CG/CST/CSAR; Uganda permit 2014-12-134).

Mosquitoes

Fourteen recently established *Ae. aegypti* colonies (2-16 laboratory generations) were chosen based on their geographical origins to best represent both the ancestral and the invasive range of the species (Table S1). Mosquitoes were reared under controlled insectary conditions (28°C, 12h:12h light:dark cycle and 70% relative humidity). Prior to performing the experiments, their eggs were hatched synchronously in a vacuum chamber for 1 hour. Their larvae were reared in plastic trays containing 1.5 liter of dechlorinated tap water and supplemented with a standard diet of Tetramin (Tetra) fish food at a density of 200 larvae per tray. After emergence, adults were kept in 30 × 30 × 30 cm BugDorm-1 insect cages (BugDorm) with permanent access to 10% sucrose solution. The gut bacterial microbiome of diverse *Ae. aegypti* colonies (including four colonies included in the present study) reared in the same insectary was remarkably similar and is therefore unlikely to be confounded with genetic effects (*45*). However, the colonies were not systematically screened for insect-specific flaviviruses, which can influence arbovirus infection (*46*). For each experiment, all the mosquito colonies were reared simultaneously in the same insectary.

Virus strains

Seven wild-type ZIKV strains (with <5 passages in cell culture) were chosen based on their geographical origin and year of isolation to best represent the current breadth of ZIKV genetic diversity (Table S2). ZIKV strains were obtained from the World Reference Center for Emerging Viruses and Arboviruses at the University of Texas Medical Branch (PRVABC59, FSS13025), the Armed Forces Research Institute of Medical Sciences (PHL/2012/CPC-0740, THA/2014/SV0127-14), the Institut Louis Malardé in French Polynesia (PF13/251013-18) and the Institut Pasteur in Dakar (Kedougou2011, Kedougou2015). Viruses were amplified in the C6/36 *Aedes albopictus* cell line (ATCC CRL-1660) to generate high-titered stocks as previously described (*47*). Their infectious titers were measured in C6/36 cells using a standard focus-

forming assay (FFA) as previously described (*47*). A commercial mouse anti-flavivirus group antigen monoclonal antibody (MAB10216; Merck Millipore) diluted 1:1,000 in phosphate-buffered saline (PBS; Gibco Thermo Fisher Scientific) supplemented with 1% bovine serum albumin (BSA; Interchim) was used as the primary antibody. The secondary antibody was an Alexa Fluor 488-conjugated goat anti-mouse antibody (A-11029; Life Technologies) diluted 1:500 in PBS supplemented with 1% BSA. The DENV-1 KDH0030A strain was isolated in Thailand in 2010 (*48*). The DENV-2 GA2_60 and the DENV-3 GA28-7 strains were isolated in Gabon in 2010 (*49*). The DENV-4 63632 strain was isolated in Senegal in 1983 (*50*). The YFV S79 strain was isolated in Senegal in 1979 (*51*).

Mouse and cell lines

C57BL/6J and 129S2/SvPas mice deficient for the interferon type I receptor (*Ifnar1*$^{tm1Agt/tm1Agt}$, knockout allele RRID MGI_1930950), noted *Ifnar1*$^{-/-}$ mice, were maintained under specific pathogen-free conditions with a 14h:10h light:dark cycle and food and water *ad libitum* at the Institut Pasteur animal facility. All of the mice were euthanized by cervical dislocation when the humane endpoints were obtained or at the end of the experiments. The *Ae. albopictus* cell line C6/36 (ATCC CRL-1660) was maintained at 28°C under atmospheric CO_2 in tissue-culture flasks with non-vented caps, in Leibovitz's L-15 medium complemented with 10% fetal bovine serum (FBS), 2% tryptose phosphate broth (Gibco ThermoFisher Scientific), 1× non-essential amino acids (Gibco ThermoFisher Scientific), 10 U/ml of penicillin (Gibco Thermo Fisher Scientific) and 10 µg/ml of streptomycin (Gibco ThermoFisher Scientific). The *Cercopithecus aethiops* cell line Vero (ATCC CCL-81) was maintained at 37°C under 5% CO_2 in tissue-culture flasks with vented caps, in Dulbecco's Modified Eagle Medium (DMEM, high glucose, GlutaMAX supplement, Gibco ThermoFisher Scientific) without sodium pyruvate and complemented with 10% FBS, 10 U/ml of penicillin, and 10 µg/ml of streptomycin.

Artificial infectious blood meals

Mosquitoes were orally challenged with ZIKV, DENV and YFV by membrane feeding as previously described (*46*). Briefly, three- to seven-day-old females deprived of sucrose solution for 24 hours were offered an artificial infectious blood meal for 15 min using a Hemotek membrane-feeding apparatus (Hemotek Ltd.) with porcine intestine as the membrane. Blood meals consisted of a 2:1 mix of washed human erythrocytes and virus suspension. To establish the dose responses, the mosquitoes were exposed to different virus concentrations by diluting the virus stocks in cell culture medium prior to preparing the artificial infectious blood meal. Adenosine triphosphate (Merck) was added to the blood meal as a phagostimulant at a final concentration of 10 mM. Fully engorged females were sorted on wet ice, transferred into 1-pint cardboard containers and maintained under controlled conditions (28°±1°C, 12h:12h light:dark cycle and 70% relative humidity) in a climatic chamber with permanent access to 10% sucrose solution. After 7 days of incubation, the mosquito bodies were homogenized individually in 300 µl of squash buffer (Tris 10 mM, NaCl 50 mM, EDTA 1.27 mM with a final pH adjusted to 8.2) supplemented with 1 µl of proteinase K (Eurobio Scientific) for 55.5 µl of squash buffer. The body homogenates were clarified by centrifugation and 100 µl of each supernatant were incubated for 5 min at 56ºC followed by 10 min at 98ºC to extract viral RNA. Detection of ZIKV RNA was performed using a two-step RT-PCR reaction to generate a 191-bp amplicon located in a conserved region of the ZIKV genome from the 3' end of the *NS1* gene to the 5' end of *NS2A* gene (forward primer [F]: 5'-GTATGGAATGGAGATAAGGCCCA-3'; reverse primer [R]: 5'-

ACCAGCACTGCCATTGATGTGC-3'). Specific primer pairs were used to detect DENV-1 (F: 5'-GGAAGGAGAAGGACTCCACA-3'; R: 5'-ATCCTTGTATCCCATCCGGCT-3'), DENV-2 (F: 5'-CTGCACAAGCTAGGCTACAT-3'; R: 5'-AGTGTCATCGGCGTACATTG-3'), DENV-3 (F: 5'- AGAAGGAGAAGGACTGCACA-3'; R: 5'-ATTCTTGTGTCCCAACCGGCT-3'), DENV-4 (F: 5'-GAAGGTCTGCATAGGTTGGGAT-3'; R: 5'-TGATTCTTGTGTCCCAGCCTG-3'), and YFV (F: 5'- GCGTAAGGCTGGAAAGAGTG-3'; R: 5'-CTTCCTCCCTTCATCCACAA-3'). The total RNA was reverse transcribed into cDNA using random hexameric primers and the M-MLV reverse transcriptase (ThermoFisher Scientific) by the following program: 10 min at 25°C, 50 min at 37°C and 15 min at 70°C. The cDNA was subsequently amplified using DreamTaq DNA polymerase (ThermoFisher Scientific). For this step, 20-µl reaction volumes contained 1× of reaction mix and 10 µM of primers. The thermocycling program was 2 min at 95°C, 35 cycles of 30 sec at 95°C, 30 sec at 60°C, and 30 sec at 72°C with a final extension step of 7 min at 72°C. Amplicons were visualized by electrophoresis on a 2% agarose gel.

Mouse-to-mosquito ZIKV transmission assay

Ten-week-old *Ifnar1*$^{-/-}$ mice were intra-peritoneally injected with a 200-µl inoculum containing 10^5 focus-forming units (FFU) of the ZIKV_Cambodia_2010 strain. From day 1 to day 7 post inoculation, mice were anesthetized daily using 80 mg/kg of ketamine and 5 mg/kg of xylazine administered by the intra-peritoneal route. During mouse anesthesia, 10 µl of blood were collected by tail incision to subsequently measure viremia. The blood sample were then diluted in 45 µl of PBS and centrifuged at 4°C for 5 min at 6,000×g for plasma separation. Plasma viremia was determined by FFA in Vero cells as previously described (*46*). Each anesthetized mouse was placed on the netting-covered top of two 1-pint cardboard boxes containing two- to four-day-old female mosquito previously deprived of sucrose solution for 24 hours. One box contained 25 female mosquitoes from Gabon while the other one contained 25 female mosquitoes from Guadeloupe. All 50 female mosquitoes were allowed to simultaneously blood feed on the same mouse for 15 min. Fully engorged females were sorted on wet ice, transferred into fresh 1-pint cardboard containers and maintained under controlled conditions (28°±1°C, 12h:12h light:dark light cycle and 70% relative humidity) in a climatic chamber with permanent access to 10% sucrose solution. After 14 days of incubation, the mosquitoes were paralyzed with triethylamine to perform *in vitro* salivation as described previously (*52*). The proboscis of each female was inserted into a 20-µl pipet tip containing 10 µl of FBS. After 30 min of salivation, the saliva-containing FBS was mixed with 30 µl of Leibovitz's L-15 medium and stored at -80°C for later testing. The saliva samples were subsequently thawed and inoculated onto C6/36 cells for ZIKV titer determinations by FFA as described above without subsequent dilution. Their bodies were homogenized and tested for ZIKV infections by RT-PCR as described above**.**

Mosquito intercrosses

In order to perform QTL mapping by bulk segregant analysis (*23*), two reciprocal crosses were set up between a ZIKV-resistant parental colony (Gabon) and a ZIKV-susceptible colony (Guadeloupe). The initial crosses were followed by several non-overlapping generations of interbreeding, and phenotypic selection was conducted only in the final generation. Intercross 1 was initiated by mixing 132 virgin females from the 10^{th} laboratory generation of the Gabon colony with 150 virgin males from the 7^{th} laboratory generation of the Guadeloupe colony.

Intercross 2 was initiated by mixing 150 virgin males from the 10th laboratory generation of the Gabon colony with 128 virgin females from the 7th laboratory generation of the Guadeloupe colony. To sex-sort the virgin individuals, the larvae from each colony were reared as described above and their pupae were individually isolated in plastic tubes prior to adult emergence. Adults were maintained in a 30×30×30 cm Bugdorm-1 insect cage as described above. During subsequent generations, the intercross progeny was maintained by mating and oviposition *en masse* of 800-1,000 adults at each generation. Intercross females of generations F_1, F_2, F_3, F_4 and F_6 were orally exposed to artificial ZIKV infectious blood meals and their ZIKV susceptibility was determined on day 7 post blood meal as described above. The head, thorax and legs of each female were used to extract genomic DNA using the NucleoSpin 96 Tissue kit (Macherey-Nagel) according to the manufacturer's instructions. The amount of DNA isolated from each individual was quantified using the Picogreen (Thermo Fisher Scientific) reagent following the manufacturer's instructions.

Restriction-site associated DNA sequencing

Twelve sequencing pools (2 reciprocal crosses × 2 phenotypes [resistant, susceptible] + 2 parental colonies, in duplicate), each consisting of 48 individuals, were prepared to perform restriction site-associated DNA sequencing (RAD-seq) according to established methods (*53*). Individual DNA concentrations were adjusted prior to pooling so that each individual contributed the same amount of DNA to the pool. A modified version of the original double-digest RAD-seq protocol (*54*) was used, as previously described (*53*). Briefly, 200 ng of DNA per pool was digested with NlaIII and MluCI restriction enzymes (New England Biolabs). The resulting digestions were cleaned with SPRI magnetic beads and barcoded using modified Illumina P1 and P2 adapters that enable unique identification of each pool. The barcoded fragments from all pools were combined, cleaned with SPRI magnetic beads and size-selected using the Blue Pippin 2% agarose kit (Sage Sciences) to retain fragments of 300-450 bp in length. The library was finalized after 10 PCR cycles using Phusion High-Fidelity PCR Master Mix (New England Biolabs) and Illumina primers, and sequenced on a NextSeq 500 instrument (Illumina) using the paired-end (2×150 bp) chemistry. Raw sequencing data were deposited to the NCBI SRA repository under accession number PRJNA640190. Sequencing data were processed (trimmed to 90 bp and filtered for phred>20) using a previously developed bash script (*53*), and the high-quality reads were aligned to the AaegL5 reference genome assembly (*55*) using Bowtie (*56*). Unambiguously mapped reads were processed in SAMtools (*57*) to generate sorted bam files, and single-nucleotide polymorphisms (SNPs) were called in ANGSD (*58*) using the likelihood-ratio test (-snp_pval 1e-6) based on the GATK model for genotype likelihood estimation (-GL 2) for SNPs with read depth ≥46× (~0.5× per individual in a pool) and ≤1,600× to exclude outliers with extreme read depth.

QTL mapping

QTL mapping was performed with the R package QTLseqr v0.7.5.2 (*44*), which relies on a *G'* statistic adapted for bulk segregant analysis with high-throughput sequencing data (*59*). The *G'* statistic is calculated for each SNP based on the observed and expected allele depths and adjusted with a tricube smoothing kernel. The smoothing allows for noise reduction and accounts for linkage disequilibrium between SNPs. *G'* was close to being log-normally distributed in both intercrosses, allowing *p* values to be estimated for each SNP using non-parametric estimation of the null distribution of *G'* (*59*). To summarize the ancestry difference between the phenotypic

pools (resistant vs. susceptible), for each biallelic SNP an ancestry difference value was calculated as $a_d=(f_R - f_S)/(p_R - p_S)$ where p_R is the frequency of the major allele in the resistant parent (Gabon), p_S is the frequency of this allele in the susceptible parent (Guadeloupe), f_R is the frequency of this allele in the resistant progeny and f_S is the frequency of this allele in the susceptible progeny (*23*). The a_d value represents the proportion of ancestry from the resistant parent in the resistant progeny and was averaged by 5-Mb moving window. The analysis of a_d was restricted to SNPs with large differences in allele frequency between the parents ($p_R - p_S \geq 0.25$).

Genetic ancestry analyses

The relationship between ZIKV susceptibility and 'domestic' genetic ancestry was analyzed using previously published information for NGO, KED, KUM, ENT, KAK and RAB colonies (*7*) and the newly generated RAD-seq data for Gabon and Guadeloupe colonies. A total of 72,721 SNPs were identified in the RAD-seq data from the Guadeloupe and Gabon colonies that had >20 reads in both colonies, were polymorphic in at least one of them, and overlapped with maximum-likelihood allele frequency estimates for wild-caught founders of the other African colonies (*7*). Signals of admixture were tested by ABBA-BABA or *D* statistics (*60*) using a block jackknife of sets of 100 consecutive SNPs to calculate *Z* scores and *p* values using known non-admixed populations (BKK, SAN, ENT, and LPV, see ref. (*7*)) as references. The null hypothesis of simple tree-like relationships was rejected for both colonies (Gabon: *Z* score=2.19; Guadeloupe: *Z* score=-3.13). Admixture proportions were estimated by the *f4* ratio, as follows: for Gabon, *f4*(SAN, KED; Gabon, LPV)/*f4*(SAN, KED; BKK, LPV); for Guadeloupe *f4*(LPV, BKK; SAN, Guadeloupe)/*f4*(LPV, BKK; KED, Guadeloupe) (*7, 60*). In the case of Guadeloupe, deviations from simple tree-like relationships were most consistent with potential past gene flow between South America and Africa, rather than admixture in Guadeloupe, so this population was designated as having fully 'domestic' ancestry.

Statistics

Statistical analyses of phenotypic data were performed using the R software version 3.5.2 (www.r-project.org) and JMP version 10.0.2 (www.jmpdiscovery.com). Graphical representations were generated with the R package *ggplot2* (*61*). The proportion of infected mosquitoes and the proportion of infectious mosquitoes were analyzed by logistic regression of the corresponding binary phenotype (ZIKV-positive=1, ZIKV-negative=0), followed by an analysis of deviance with the R package *car* (*62*) or likelihood-ratio χ^2 tests in JMP. For dose-response analyses of infection rates, the logistic model included the infectious dose ($\log_{10}$-transformed blood meal titer) as a covariate and the OID_{50} and OID_{75} values and their respective 95% confidence intervals were derived from the logistic fits. The effect of the mosquito population on infection and transmission rates in mouse experiments were analyzed for each time point and each mouse strain separately using replicate mouse as a covariate. The replicate mouse × population interaction was removed from the model because it was always statistically non-significant ($p>0.05$). The potential influence of the number of laboratory generations on ZIKV susceptibility was assessed by analysis of variance of OID_{50} estimates including the virus strain as a covariate.

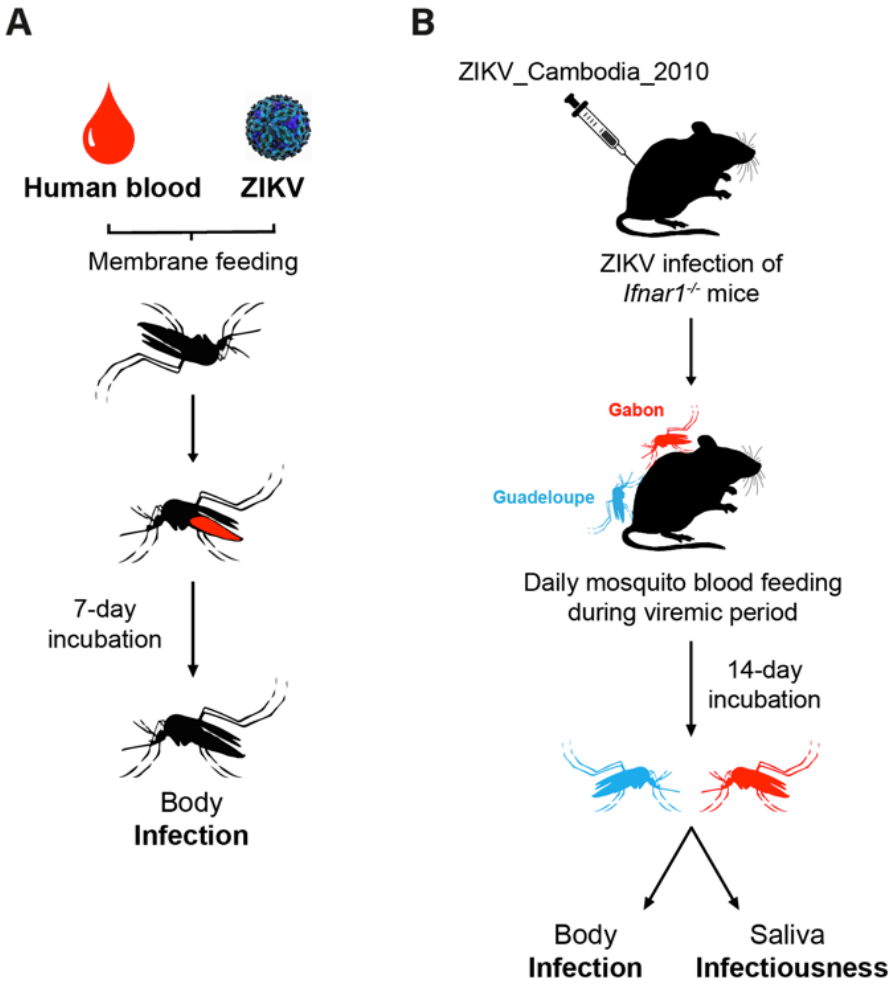

Fig. S1.

Experimental infections of mosquitoes. **A**. Flowchart of the membrane-feeding assay to measure ZIKV, DENV and YFV susceptibility. **B**. Flowchart of the mouse-to-mosquito ZIKV transmission assay.

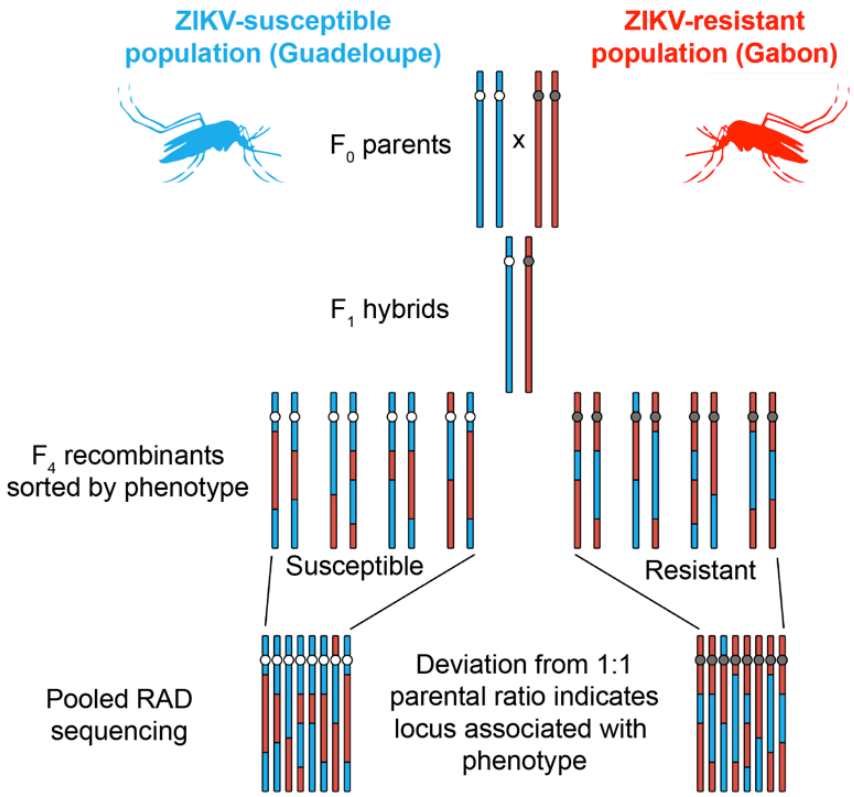

Fig. S2.

Genetic mapping strategy. Flowchart of the QTL mapping strategy based on the intercross between a ZIKV-resistant parent from Gabon and a ZIKV-susceptible parent from Guadeloupe, followed by bulk segregant analysis. The white circle represents a hypothetical susceptibility locus and the grey circle represents a hypothetical resistance locus.

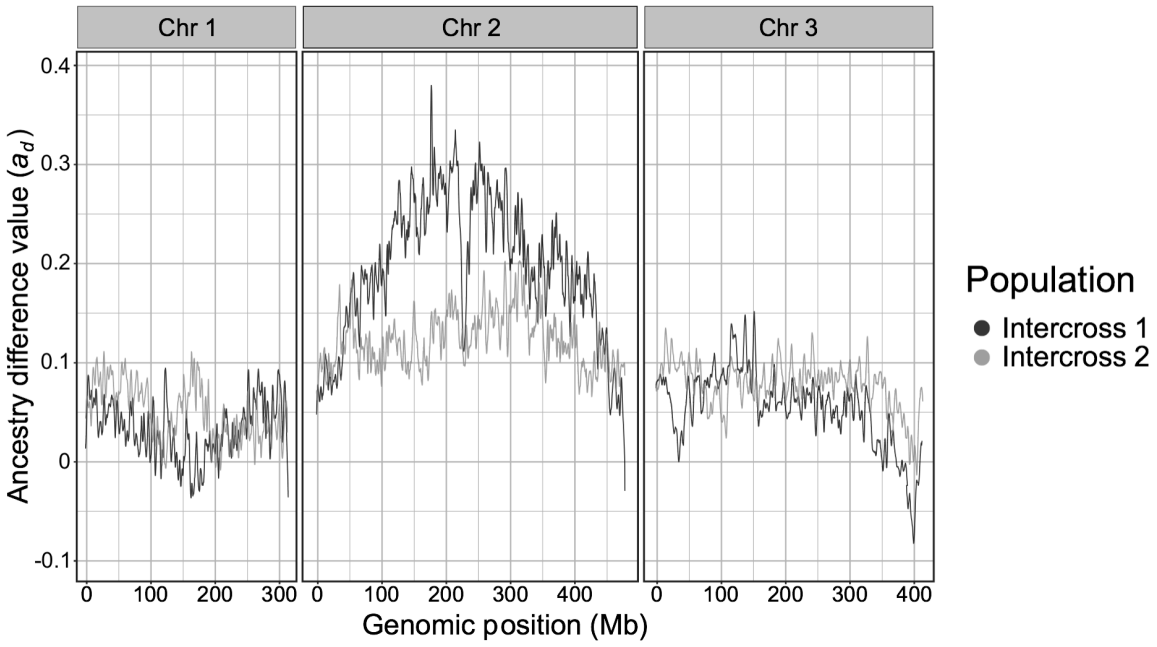

Fig. S3.

Ancestry difference between phenotypic pools in the intercross progeny. The ancestry difference (a_d) value represents the proportion of ancestry from the resistant parent in the resistant progeny and is shown in the two reciprocal intercrosses as the average by 5-Mb moving window for SNPs whose difference in allele frequency was ≥25% between the resistant (Gabon) and susceptible (Guadeloupe) parents.

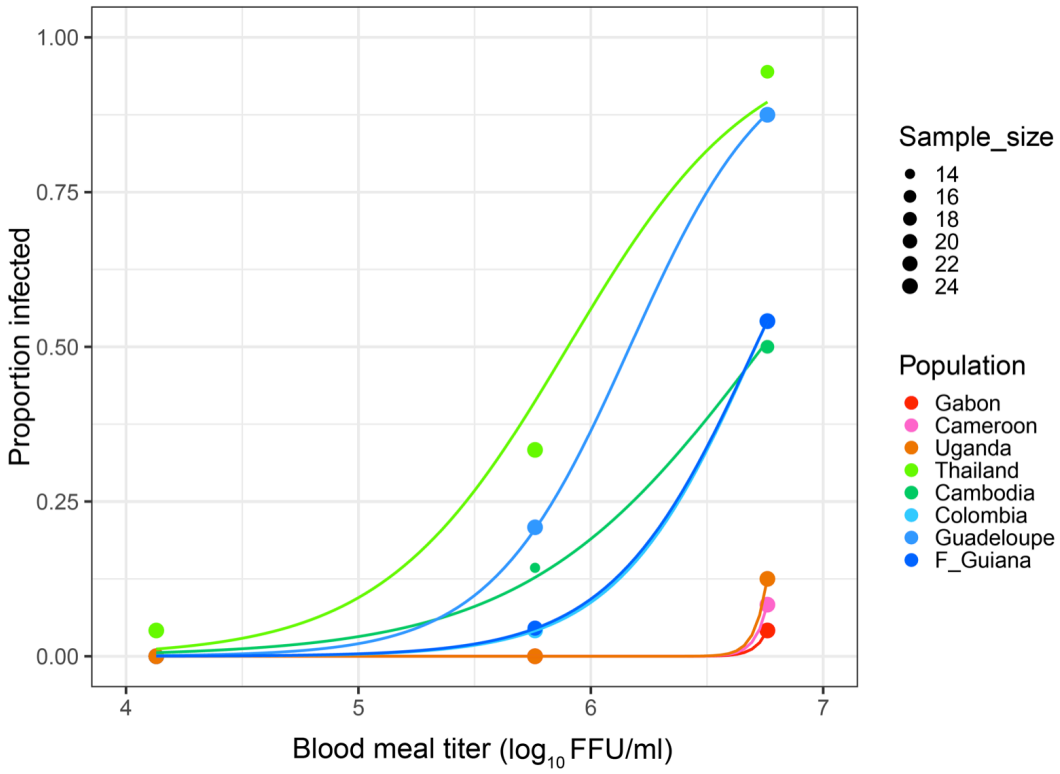

Fig. S4.

Dose-response curves of eight field-derived *Ae. aegypti* colonies orally challenged by YFV. The proportions of YFV-infected mosquitoes 7 days post infectious blood meal are shown as a function of the blood meal titers in $\log_{10}$-transformed focus-forming units (FFU)/ml. The lines represent the logistic regression results.

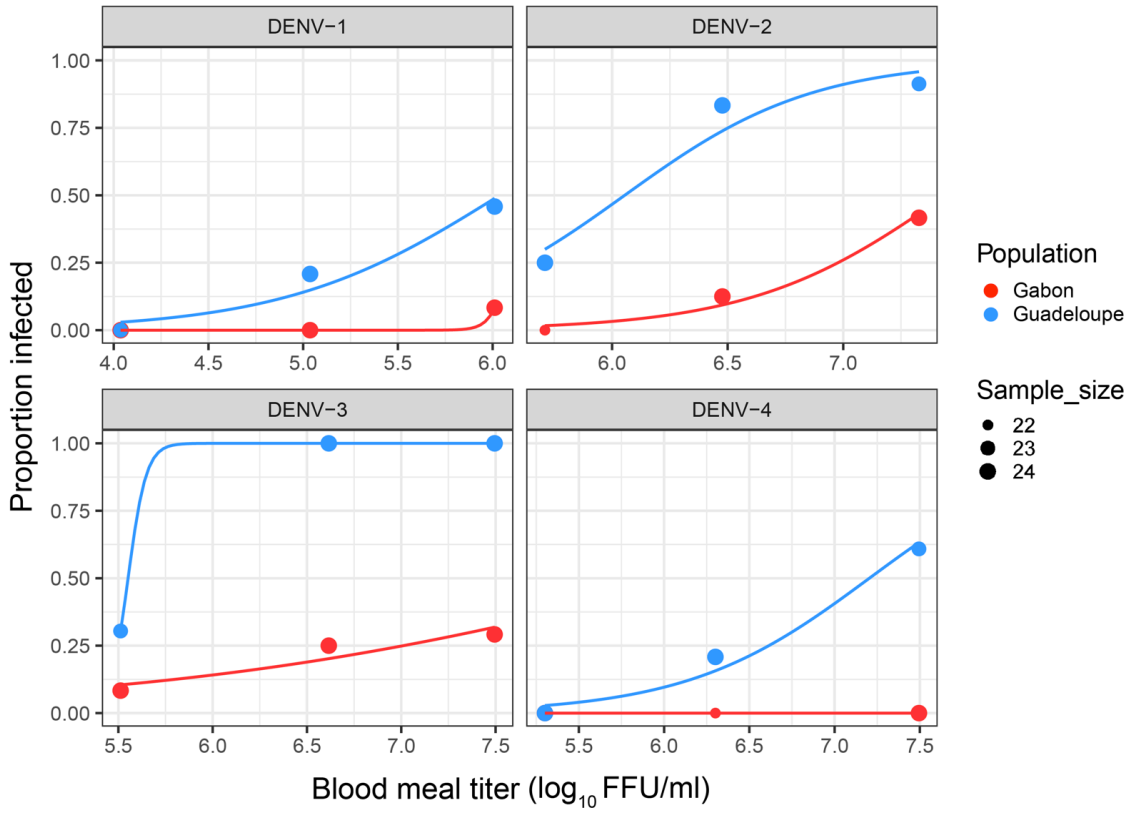

Fig. S5.

Dose-response curves of *Ae. aegypti* colonies from Gabon and Guadeloupe orally challenged by the four DENV types. The proportions of DENV-infected mosquitoes 7 days post infectious blood meal are shown as a function of the blood meal titers in $\log_{10}$-transformed focus-forming units (FFU)/ml. The lines represent the logistic regression results.

Table S1.

Aedes aegypti colonies included in this study. The names of the mosquito colonies used in the study, their country of origin, locality, year of collection and number of generations spent in the laboratory prior to this study are shown. The percentage of 'domestic' genetic ancestry (% *Aaa*) was inferred from the whole-genome sequences of the wild-caught progenitors or from RAD-seq data generated from colonized individuals (*). Und=undetermined.

Name in this study	Country	Locality	Year	Generation	% *Aaa*
Thailand	Thailand	Kamphaeng Phet	2013	13-14	Und
Cambodia	Cambodia	Phnom Penh	2015	8-9	Und
Colombia	Colombia	Barranquilla	2017	2-3	Und
F_Guiana	French Guiana	Cayenne	2015	5-6	Und
Guadeloupe	Guadeloupe	Saint François	2015	6-13	100*
Gabon	Gabon	Lopé	2014	9-16	7.30*
Uganda	Uganda	Zika	2016	4-5	Und
Cameroon	Cameroon	Bénoué	2014	7-8	Und
NGO	Senegal	Ngoye	2018	5	37.4
KED	Senegal	Kédougou	2018	4	0.86
KUM	Ghana	Kumasi	2018	4	6.75
KAK	Kenya	Kakamega	2017	6	1.66
RAB	Kenya	Rabai	2017	6	7.36
ENT	Uganda	Entebbe	2015	12	0.00

Table S2.

ZIKV strains included in this study. The name of the ZIKV strains with their country of origin, original strain name, source of isolation, year of collection and the passage history prior to use in this study are indicated. TS: *Toxorhynchites splendens* mosquitoes; C6/36: *Aedes albopictus* cells; Vero: green monkey kidney cells; SM: suckling mouse brains.

Name in this study	Country	Strain ID	Source	Year	Passage history
ZIKV_F_Polynesia_2013	French Polynesia	PF13/251013-18	Human serum	2013	C6/36-4
ZIKV_Puerto_Rico_2015	Puerto Rico	PRVABC59	Human serum	2015	Vero-2; C6/36-3
ZIKV_Philippines_2012	Philippines	CPC-0740	Human serum	2012	TS-1; C6/36-2; Vero-1; C6/36-1
ZIKV_Thailand_2014	Thailand	SV0127-14	Human serum	2014	TS-1; C6/36-2; Vero-1; C6/36-1
ZIKV_Cambodia_2010	Cambodia	FSS13025	Human serum	2010	Vero 2; SM-1; C6/36-1
ZIKV_Senegal_2011	Senegal	Kedougou2011	Pool of *Aedes* spp. and *Mansonia* spp.	2011	C6/36-2
ZIKV_Senegal_2015	Senegal	Kedougou2015	Pool of *Aedes* spp. and *Mansonia* spp.	2015	C6/36-2

Table S3.

ZIKV susceptibility of *Aedes aegypti* colonies included in this study. The table shows the estimated 50% oral infectious dose (OID_{50}) values and their 95% confidence intervals derived from the logistic fits of the dose-response curves and expressed in log_{10}-transformed focus-forming units (FFU)/ml. Und=undetermined; NT=not tested.

Mosquito colony	ZIKV_Cambodia_2010	ZIKV_Philippines_2012	ZIKV_F_Polynesia_2013	ZIKV_Thailand_2014	ZIKV_Puerto_Rico_2015	ZIKV_Senegal_2015	ZIKV_Senegal_2011
Cambodia	6.12 (5.53 – 6.80)	6.18 (5.77 – 6.52)	6.50 (6.25 – 6.76)	5.20 (4.81 – 5.54)	6.05 (5.54 – 6.33)	5.38 (Und – 5.85)	NT
Cameroon	7.19 (6.89 – 8.02)	7.00 (6.71 – 7.37)	6.83 (6.59 – 7.09)	6.34 (5.97 – 6.97)	6.98 (6.65 – 7.33)	6.55 (6.03 – 7.97)	NT
Colombia	5.50 (4.36 – 6.05)	5.85 (5.56 – 6.12)	6.84 (6.59 – 7.18)	6.13 (5.81 – 6.54)	6.05 (5.32 – 6.43)	Und	NT
F_Guiana	5.14 (3.52 – 5.68)	5.25 (4.08 – 5.61)	6.03 (5.68 – 6.36)	4.92 (4.63 – 5.19)	5.99 (5.36 – 6.29)	5.19 (Und – 5.84)	NT
Gabon	8.10 (7.26 – Und)	7.29 (7.08 – 7.55)	7.18 (6.91 – 8.27)	6.29 (5.87 – 7.12)	7.37 (7.04 – 7.78)	6.84 (6.48 – 7.68)	6.29 (5.96 – 6.59)
Guadeloupe	4.83 (2.71 – 5.37)	Und	5.83 (5.51 – 6.11)	4.73 (3.83 – 5.16)	5.08 (Und – 5.97)	5.69 (3.87 – 5.96)	5.56 (Und – 5.68)
Thailand	6.04 (5.71 – 6.33)	6.13 (5.83 – 6.39)	6.30 (5.99 – 6.64)	4.98 (4.07 – 5.44)	6.19 (5.50 – 6.56)	4.88 (Und – 5.69)	NT
Uganda	7.65 (7.10 – Und)	7.16 (6.93 – 7.43)	7.82 (7.04 – Und)	6.79 (6.72 – Und)	7.75 (7.14 – 9.09)	6.59 (6.21 – 7.04)	NT
NGO	6.32 (Und – 7.04)	NT	NT	NT	NT	NT	4.92 (Und – 5.61)
KED	7.94 (7.49 – 8.74)	NT	NT	NT	NT	NT	6.20 (5.73 – 6.59)
KUM	7.45 (7.04 – 7.97)	NT	NT	NT	NT	NT	5.89 (5.45 – 6.19)
KAK	7.66 (7.26 – 8.36)	NT	NT	NT	NT	NT	5.56 (3.95 – 6.03)
RAB	6.99 (6.27 – 7.47)	NT	NT	NT	NT	NT	5.85 (5.35 – 6.13)
ENT	7.61 (7.06 – 8.40)	NT	NT	NT	NT	NT	5.56 (4.48 – 5.91)

Table S4.

QTL mapping results. The table shows the statistically significant QTL detected in the two reciprocal intercrosses, their genomic position, SNP density, and *G'* summary statistics.

Intercross	Chr	Start	End	Length	No. SNPs	Mean no. SNPs/Mb	Max *G'*	Position Max *G'*	Mean *G'*	Std. dev. *G'*	Mean *p* value	Mean *q* value
1	2	128307858	189268199	60960341	12605	207	11.90362	174220367	9.98161	0.64340	2.91E-05	0.000681
1	2	199321667	200588341	1266674	315	249	8.99794	200141717	8.96851	0.01793	9.03E-05	0.000975
1	2	208222803	221309132	13086329	2919	223	10.55020	218672721	9.63389	0.37708	3.87E-05	0.000714
1	2	239380068	250368015	10987947	2756	251	10.60863	244607604	9.77163	0.49641	3.57E-05	0.000709
1	2	266331252	282747300	16416048	3243	198	9.33820	277970508	9.16086	0.08385	6.83E-05	0.000864
2	2	37047085	37135634	88549	33	373	3.85928	37092592	3.85673	0.00163	0.002061701	0.049001
2	2	284547688	306776528	22228840	4304	194	4.38860	300209720	4.09978	0.13919	0.000623971	0.023462
2	2	309872477	332550739	22678262	4102	181	4.64790	326149498	4.21929	0.19776	0.000447625	0.020022
2	2	337389780	344844034	7454254	1403	188	4.11790	340953347	3.98689	0.07804	0.001035143	0.031122

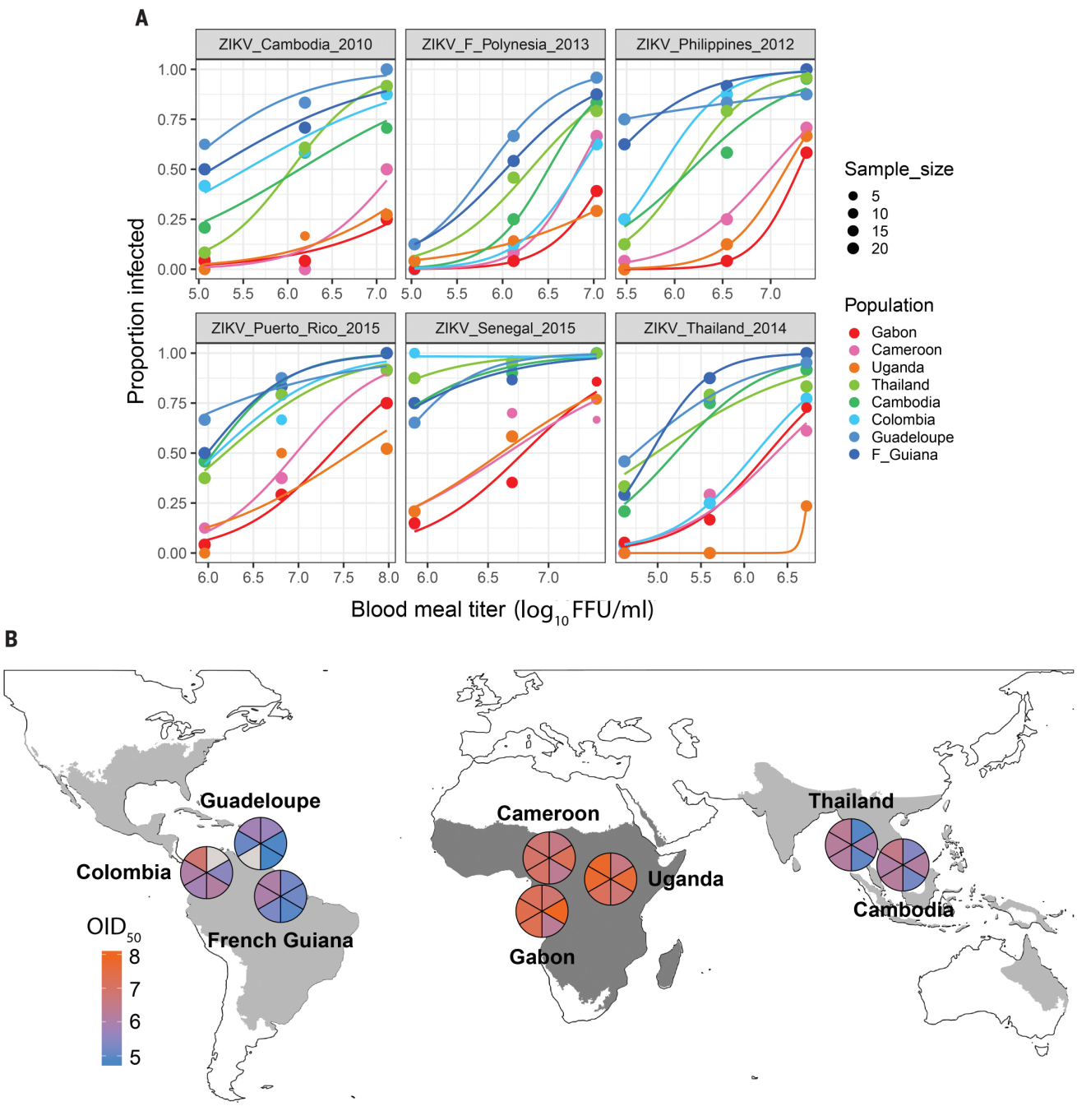
A
ZIKV_Cambodia_2010
ZIKV_F_Polynesia_2013
ZIKV_Philippines_2012
ZIKV_Puerto_Rico_2015
ZIKV_Senegal_2015
ZIKV_Thailand_2014
Proportion infected
Blood meal titer (log10FFU/ml)
Sample_size
5
10
15
20
Population
Gabon
Cameroon
Uganda
Thailand
Cambodia
Colombia
Guadeloupe
F_Guiana
B
Guadeloupe
Colombia
French Guiana
Cameroon
Uganda
Gabon
Thailand
Cambodia
OID50
8
7
6
5

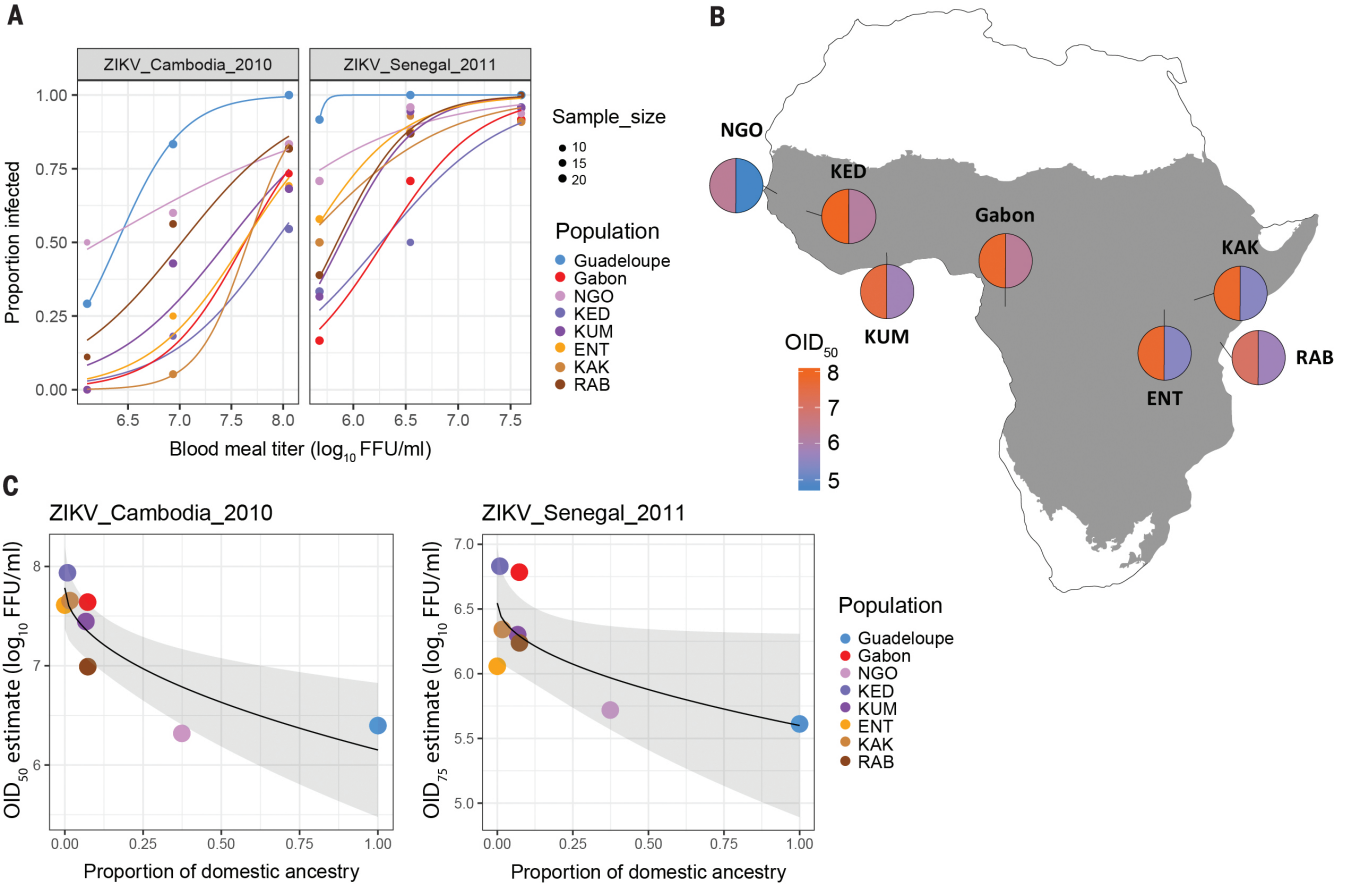
A
ZIKV_Cambodia_2010
ZIKV_Senegal_2011
Proportion infected
1.00
0.75
0.50
0.25
0.00
6.5
7.0
7.5
8.0
6.0
6.5
7.0
7.5
Blood meal titer (log10 FFU/ml)
Sample_size
10
15
20
Population
Guadeloupe
Gabon
NGO
KED
KUM
ENT
KAK
RAB
B
NGO
KED
Gabon
KAK
KUM
ENT
RAB
OID50
8
7
6
5
C
ZIKV_Cambodia_2010
ZIKV_Senegal_2011
OID50 estimate (log10 FFU/ml)
OID75 estimate (log10 FFU/ml)
8
7
6
7.0
6.5
6.0
5.5
5.0
0.00
0.25
0.50
0.75
1.00
Proportion of domestic ancestry
Proportion of domestic ancestry
Population
Guadeloupe
Gabon
NGO
KED
KUM
ENT
KAK
RAB

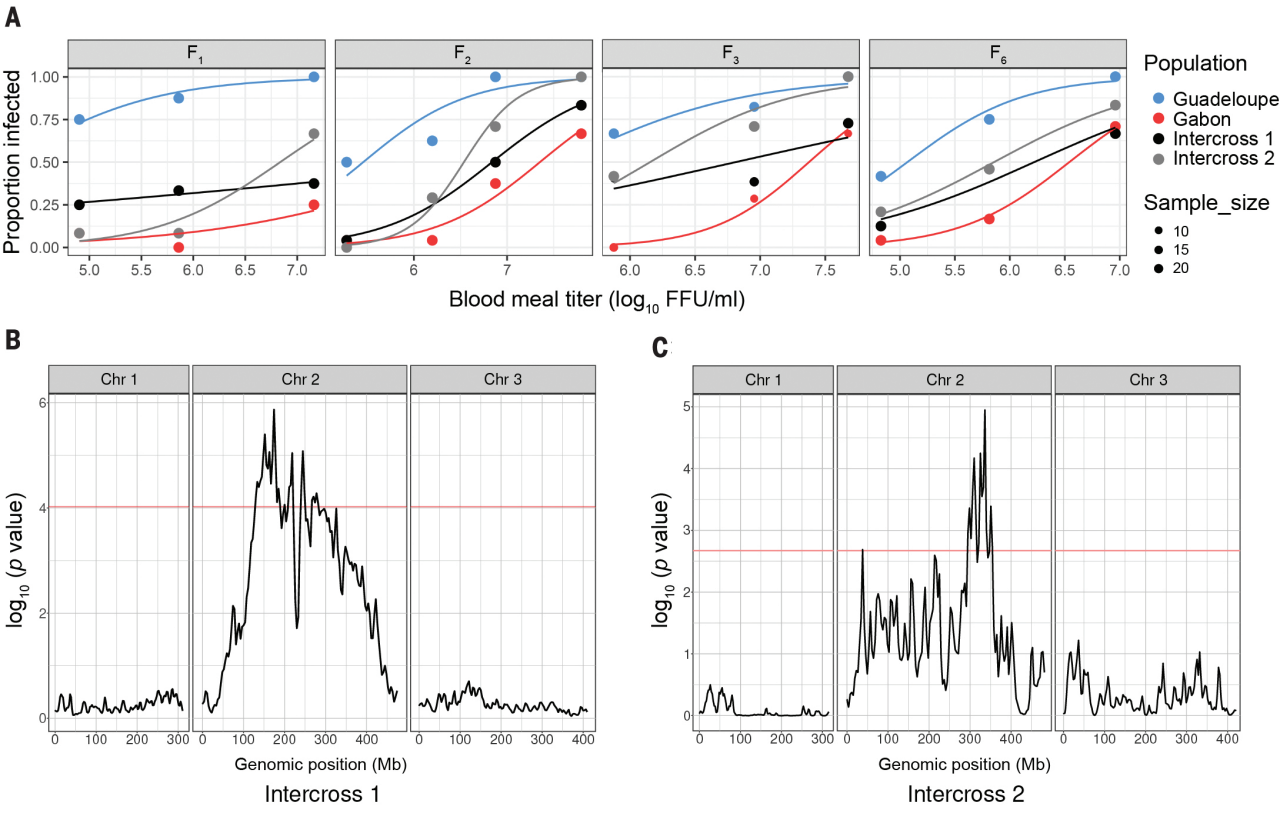
A
F1
F2
F3
F6
Proportion infected
Blood meal titer (log10 FFU/ml)
Population
Guadeloupe
Gabon
Intercross 1
Intercross 2
Sample_size
10
15
20
B
Chr 1
Chr 2
Chr 3
log10 (p value)
Genomic position (Mb)
Intercross 1
C
Chr 1
Chr 2
Chr 3
log10 (p value)
Genomic position (Mb)
Intercross 2

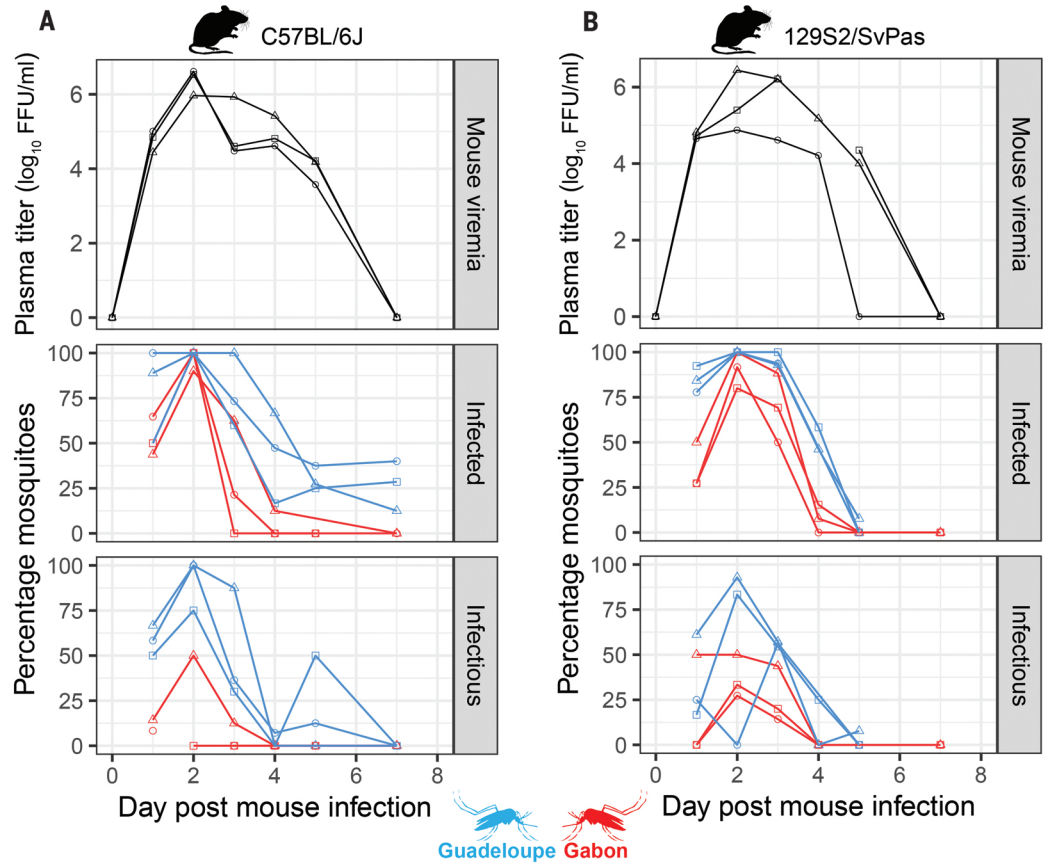
A
C57BL/6J
B
129S2/SvPas
Plasma titer (log_{10} FFU/ml)
Mouse viremia
Percentage mosquitoes
Infected
Infectious
Day post mouse infection
Guadeloupe
Gabon